Study of partial oxidation of Cu clusters by HRTEM

J. Urban, H. Sack-Kongehl and K. Weiss

Fritz-Haber-Institut der Max-Planck-Gesellschaft, Abt. Anorganische Chemie, Faradayweg 4-6, D-14195 Berlin, Germany

Received 12 July 1997; accepted 19 September 1997

Cu clusters of diameters less than 10 nm were selected as models to study oxidation as a function of size, chemical composition, and structure. The investigations were performed with high-resolution electron microscopy. It was shown that beginning with multiply twinned particles as stable structures for particles with diameters less than 5 nm and of cuboctahedra for larger particles, in the transitional state between pure metal and oxide both states can coexist within the same particle; this latter can be proved by HRTEM. It was also demonstrated that this is due to incorporating distortions as step dislocations within grain boundaries which can be shown in electron micrographs of high resolution better than 0.18 nm after image processing. The creation of sub-oxides with less reactivity than the pure metal clusters could also be demonstrated leading to morphologies which are different from those of the pure metal.

Keywords: high-resolution electron microscopy, clusters and nano materials, reactivity, sub-oxides, oxides, image processing, lattice distortions

1. Introduction

Recently, the characteristic properties of small particles in nanometer sizes (less than 50 nm diameter) have become the focus of increasing interest. Initially, these particles were of interest because they bridge the transitional state between atomic/molecular and solid state. The particles serve as nucleus for the creation of nanophase materials and nano composites and have gained importance because of their unusual mechanical, electrical, optical and magnetic properties. The incorporation of strain and its investigation is also of certain interest [1]. Since the surface/volume ratio increases with decrease in particle size these structures can serve as models for pure surfaces and are of interest as model catalysts [2–4]. Nanostructured metal clusters have a special impact in catalytic applications. They very often serve as precursors for new types of heterogeneous catalysts. They may offer substantial advantages with respect to lifetime, activity, and selectivity for chemical reactions and electrocatalysis (fuel cells). It is the aim of the present paper to demonstrate the technique of HRTEM as a tool to determine the structures and their distortions and also to study the reactivity as function of size, structure, and composition with respect to oxidation. The present study mainly focuses on the transition between the pure Cu metal and the completely oxidised state of Cu_2O.

2. Experimental and data processing

The preparation of copper and copper-oxide clusters in the size range between 1 and 10 nm diameter was performed by using the inert gas aggregation technique [5,6]. The employed experimental set-up is described in detail elsewhere [7,8]. Aside from preparing pure Cu clusters under liquid-nitrogen-cooled argon atmosphere (Linde, Argon 5.0) at 1 mbar partial pressure, also oxide clusters were prepared by adding pure oxygen (Messer Griesheim, Oxygen 4.8) to the argon gas at different partial pressures. Seeing that we were mainly interested in transitional states, i.e., states between pure copper and pure oxide as cuprite, the main focus is on the results in relation with 10^{-1} mbar partial pressure of oxygen; these preparation conditions turned out to be most suitable for the creation of such particles. Copper (Alfa, copper wire, 99.9% purity, 1 mm diameter, m3N5) was evaporated from a Knudsen cell and the clusters thus obtained were deposited on amorphous carbon films prepared by electron beam evaporation of about 3 nm thickness [9]. The cluster deposition rate was monitored by a quartz micro-balance (Inficon XTM). Typical deposition rates were measured as less than 0.1 nm/s and the deposition time was of the order of 1–3 s in order to avoid effects of coagulation on the carbon substrate. The samples were transferred under argon gas within a transfer system for structural investigations in the electron microscope. The transfer system served also as reaction chamber. High-resolution transmission electron microscopy (HRTEM) was performed with a Philips 200 kV microscope, CM200 FEG, $C_s = 1.35$ mm, with a resolution of better than 0.18 nm. To study the different steps of the partial oxidation of the clusters, the clusters were exposed to air at room temperature for different time periods after transferring the samples again from the microscope to the transfer system. Afterwards, they were again observed in the microscope.

For further interpretations of the images, the obtained EM pictures were digitised in pixel sizes of

about 0.03 nm and then image processed in order to enhance contrasts and to determine structure, lattice parameters, chemical composition and distortions as function of size and morphology of the samples. Important information on structure, symmetry, and lattice spacings can also be obtained from the power spectrum (PS), i.e., square of the Fourier transform of the images. The digitisation was performed by means of a densitometer (Image Science Software GmbH, Berlin) equipped with a CCD camera. This technique also allows to reveal distortions in grain boundaries between different areas in the clusters or layers grown epitaxially with the substrate [10] which are often due to interfaces of different compositions in the same sample. The different techniques for the image processing are described in detail elsewhere [11,12]. Computer simulations using the multi-slice technique [13] served for the interpretation of the structures. The experimentally obtained images were compared with tilt-series computed by this technique [14]. However, seeing that all images are projections, the suggested reconstructions are not always unique.

3. Results and discussion

All data, i.e., lattice parameters, lattice angles, and diameters of the particles of different preparation discussed in the following text are summarised in table 1.

3.1. Preparation without O_2

For diameters of less than 5 nm, the particles showed always the structure of icosahedra and decahedra which at times showed small lattice deformation; these latter are likely to be due to inserting internal strain in order to grow such structures [8]. Larger particles always showed the fcc bulk structure with small distortions or twinning depending on the sizes. Two examples of such species are shown in figures 1 and 2.

Figure 1 shows a Cu icosahedron oriented with respect to the substrate along the three-fold axis. The diameter of the particle is 4.7 nm. The PS shows a three-fold splitting for the three pairs of 111 reflections. The lattice spacing $d_{111} = 0.209$ nm for all segments of the 20 deformed tetrahedral sub-units which is very close to the

Table 1
Structural data of Cu and oxide clusters

Fig. No.	Material/structure	$2R$ (nm)	$h\,k\,l$	d (nm)	Angles (deg)
	Cu fcc		1 1 1	0.2087	(−11−1, −111) 70.5
			2 0 0	0.1808	(−111, 002) 54.7
	Cu_2O cuprite		1 1 1	0.2465	(−11−1, −111) 70.5
			1 1 0	0.3019	(−11−1, −110) 35.3
			2 0 0	0.2135	(−111, 002) 54.7
	CuO tenorite		0 0 2	0.2530	(002, −111) 65.9
			−1 1 1	0.2522	
1	Cu, icosahedron, three-fold axis	4.7	1 1 1	0.209	(111-segments) 60.0
2	Cu, cuboctahedron, twin	8.1			
	[1 −1 0]		1 1 1	0.211	(111, 11−1) 72.0
			1 1 −1	0.215	
	[−110]		0 0 2	0.185	(111, 11−1) 70.4
			1 1 1	0.211	(002, 111) 54.8
			1 1 −1	0.215	
3	sub-oxide, cubic [001]	4.1	2 0 0	0.183	(200, 020) 90.0
			0 2 0	0.183	
4	transition	4.2			
	Cu		1 1 1	0.209	0
	Cu_2O		1 1 1	0.243	
6	transition	4.7			
	?		?	0.218	2
	?		?	0.253	
8	Cu_2O cuprite [110]	3.4	0 0 2	0.218	(00−2, −11−1) 55.0
			−1 1 −1	0.244	(002, −111) 55.5
			−1 1 1	0.244	(−11−1, −111) 69.5
			−1 1 0	0.296	
9	transition	2.7			
	CuO tenorite [110]		−1 1 1	0.256	(−111, 002) 68.0
			0 0 2	0.265	
	Cu_2O cuprite [110]		−1 1 −1	0.237	(−11−1, −111) 71.5
			−1 1 1	0.237	
			−1 1 0	0.292	

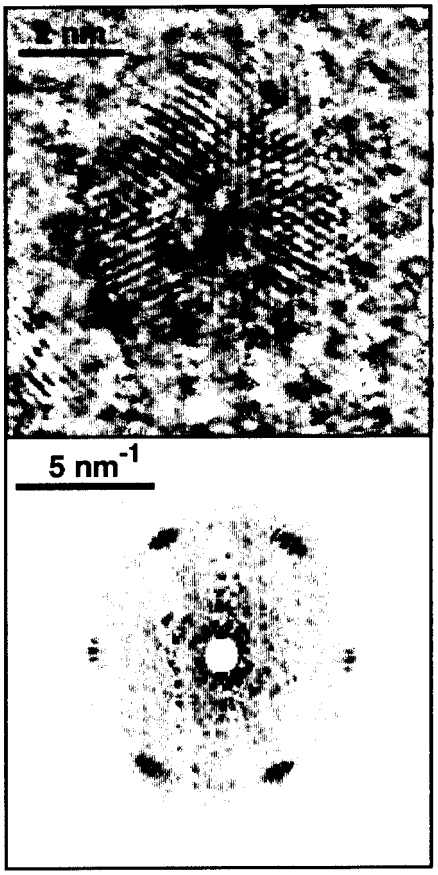

bulk fcc-value. This means that the strain is uniformly distributed across the 20 deformed tetrahedral sub-units. If the strain would not be uniformly distributed, the three pairs of the 111 reflections in the PS originating from different sub-units would be unequal which sometimes could be observed. From the three identical d_{111}-values the two bond lengths which are characteristic for icosahedra or decahedra are calculated [8]. According to ref. [8] x_1 and x_2 can be calculated for icosahedra from d_{111} as follows:

$$x_1 = d_{111}/[\alpha \cos(\varphi/2)]\,,$$

with $\alpha = a/\sqrt{2}$ which is the nearest neighbour distance for fcc bulk, $\varphi = 72^\circ$ which represents the segment angle, and

$$x_2 = x_1 \sin(\varphi/2)/[4\sin^2(\varphi/2) - 1]^{1/2}\,.$$

It was obtained as $x_1 = 0.258$ nm (+1%) and $x_2 = 0.246$ nm (−3.9%) compared to the bulk value of $x_1 = x_2 = a/\sqrt{2} = 0.256$ nm. The numbers in parentheses give the deviations from the bulk data in percent.

Figure 1. Cu, icosahedron viewed along the three-fold axis. The PS is shown in the lower part.

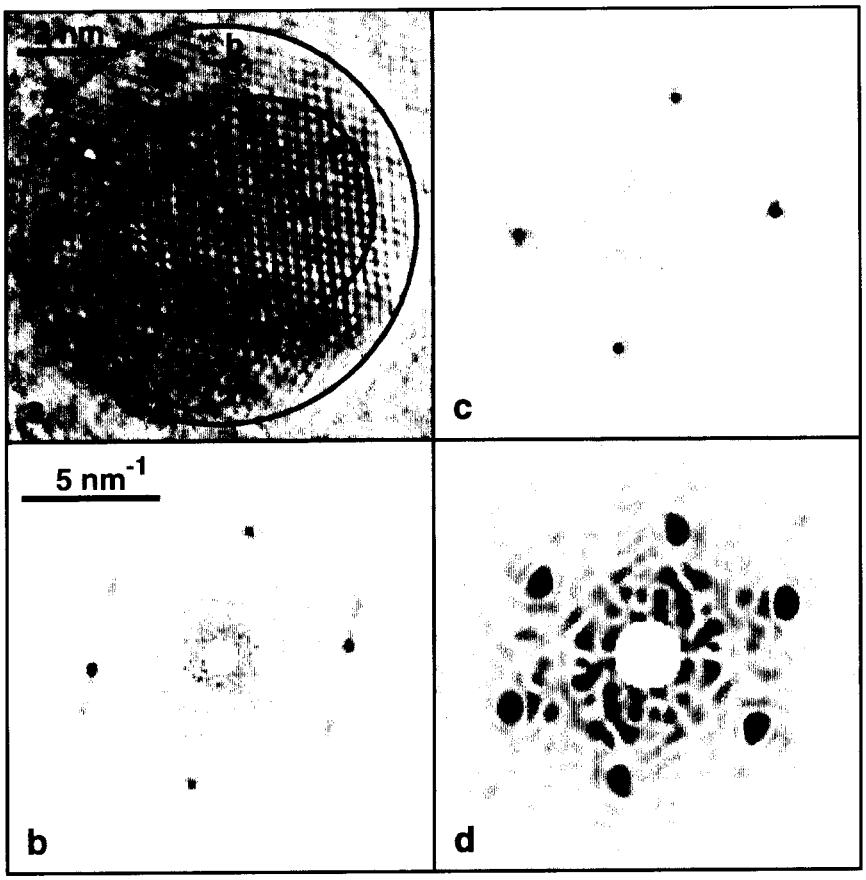

Figure 2. Cu, twinned cuboctahedron in the [1−10]- and [−110]-orientations. The different regions in the unfiltered image are encircled in (a). (b) Ps of the unfiltered particle. (c) PS of the larger region. (d) PS of the smaller region.

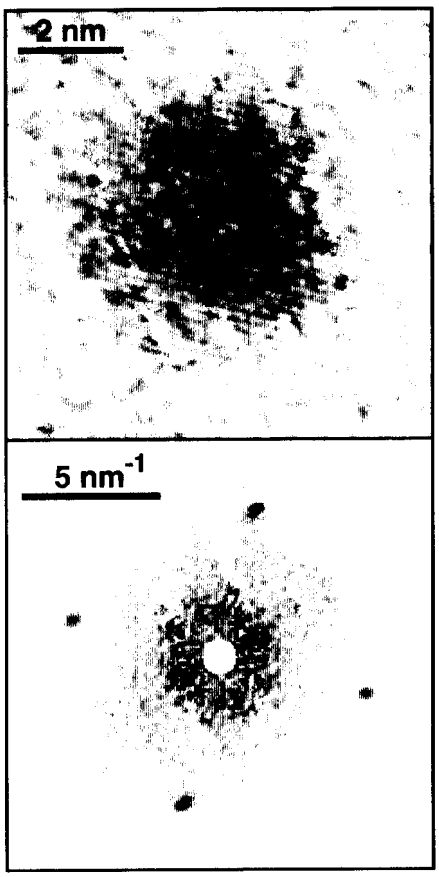

Figure 3. Cubic structure in the [001]-orientation. Sub-oxide consisting of small amounts of oxygen. The PS is shown in the lower part.

Figure 2 shows a twinned Cu particle with fcc structure in the [1 −10]- and [−110]-orientation. Here, the twin plane is the (111)-plane. The diameter of the particle is 8.1 nm. Apart from the twinning, the particle shows distortions which can be seen from the different data of the 111 and 11 −1 reflections presented in table 1.

3.2. Preparation with 10^{-1} mbar partial pressure of O_2

Figure 3 shows an example of a preparation with 10^{-1} mbar partial pressure of O_2. The particle has a diameter of 4.1 nm, the structure is fcc and the orientation is [001]. The (200) and (020) lattice parameters of $d_{200} = d_{020} = 0.183$ nm represent the corresponding lattice parameter of Cu bulk of $d_{200} = 0.181$ nm. The assumption is that the fcc structure instead of icosahedral or decahedral structure for Cu clusters of this size is due to the incorporation of small amounts of O_2 which stabilises the cubic structure even though it remains undetected in the microscope nor does it change the Cu lattice parameter dramatically seeing that the small deviation from the bulk value lies within experimental errors. However, most particles showed transitional stages between pure Cu and Cu_2O with grain boundaries which could clearly be identified after image processing by step dislocations. One example thereof is displayed in figure 4. The particle shows two different regions which can be identified by the individual backtransforms of the Fourier transforms of the images for the two reflection pairs.

From the PS shown in figure 4b two reflection pairs are observed in the same direction which represent the 111 reflections of Cu fcc and Cu_2O cuprite. The two different netplanes are parallel to each other. After filtering and backtransform, two different regions are obtained, i.e., e for Cu and f for Cu_2O. The two regions fit together exhibiting three step dislocations as shown in figure 4c, which are due to the different lattice parameters of the individual regions.

By performing computer simulations the state described in the example of figure 4 can be explained (figure 5). By adding two different regions with lattice planes parallel to each other but with different constants with soft overlaps at the interface, step dislocations are created which are imaged in figure 5c.

3.3. Preparation without O_2 but after air exposure

After exposure of the samples to air without O_2 preparation, partial oxidation processes can be observed depending on the exposure time. Figure 6 gives an example of a transitional state after 26 h of air exposure at room temperature. Cu and Cu_2O 111 reflections are split. Their directions deviate by a few degrees (about 2°) from each other. Again, the image of the total particle shown in figure 6a is Fourier transformed and the PS is given in figure 6b. After filtering, cf. figure 6d, the backtransform is shown in figure 6c. Figures 6e and 6f show the backtransforms of the individual Fourier transforms of the images, i.e., Cu in figure 6e and Cu_2O in figure 6f, respectively. Here, both backtransforms represent the same region with slightly tilted netplanes which give rise to the distortions displayed in figure 6c. This state can be explained as Moiré pattern and demonstrated with computer simulations, as is shown in figure 7. Obviously, the core of the particle still consists of Cu while the outer shell is already oxidised. This means, the particle can be described as layered structure resulting in the observed Moiré pattern. The slight tilt of the different layers by about 2° may be due to the match of the different layers of different lattice constants.

The oxidation process is fully terminated for pure Cu particles in the investigated size range after about 100 h of air exposure if the preparation was performed without O_2. An example is shown in figure 8. Here, a Cu_2O cuprite particle in the [110]-orientation is shown. To a certain degree the particle is distorted which is monitored by the deviation of the lattice parameters calculated from the PS from the bulk values.

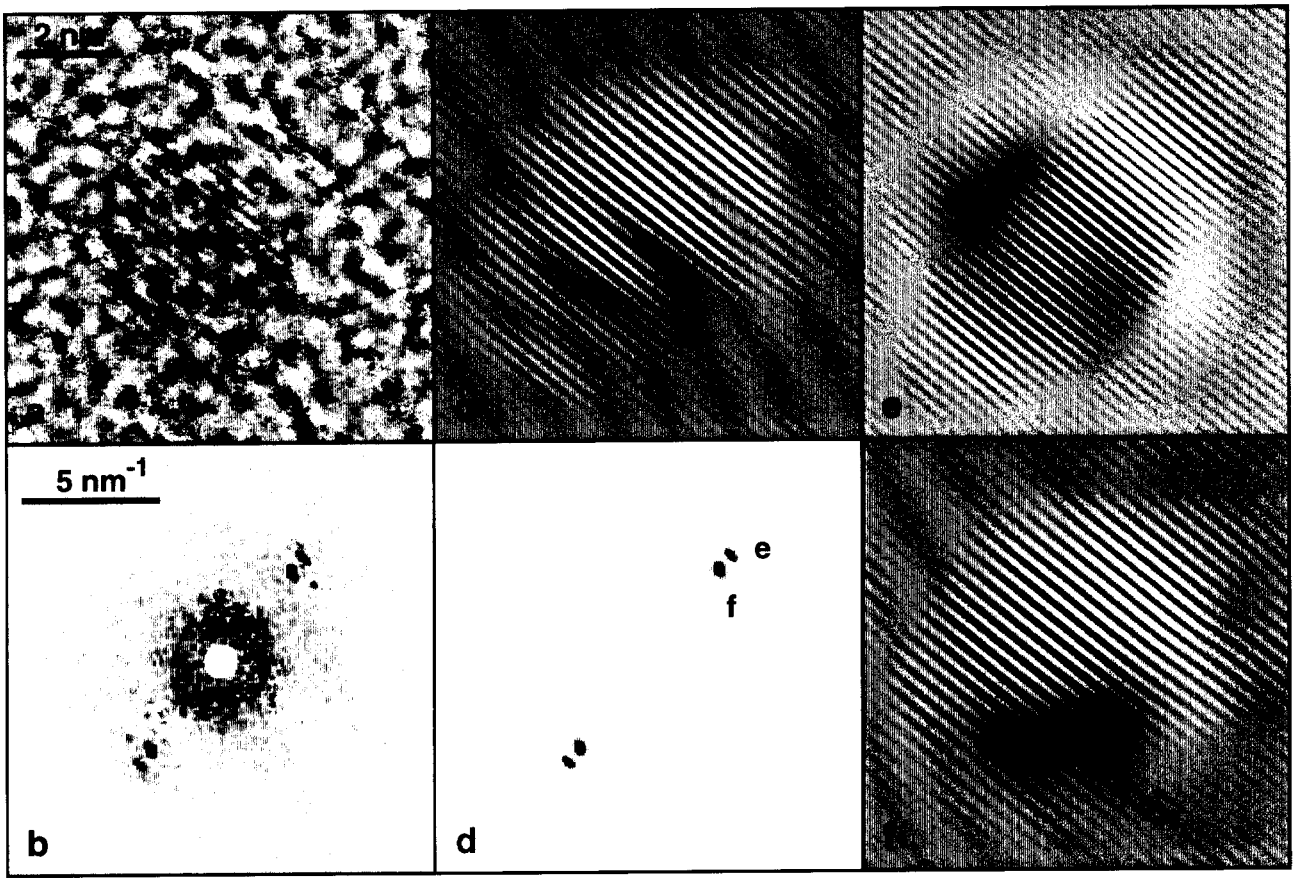

Figure 4. Transition between Cu (cubic) and Cu_2O consisting of two separated regions. (a) Image of the unfiltered particle. (b) PS of the unfiltered particle. (c) Filtered image with three step dislocations. (d) PS of the filtered image. (e) Backtransform of the Cu region. (f) Backtransform of the oxide region.

3.4. Preparation with oxygen and storage in air at room temperature

The situation for preparations with O_2 is different from those without oxygen with respect to oxidation through air contamination. This means that the reactivity of these particles is deteriorated. This is demonstrated in an example displayed in figure 9.

Figure 9 shows a particle prepared with 2×10^{-3} mbar O_2 partial pressure and storage in air for

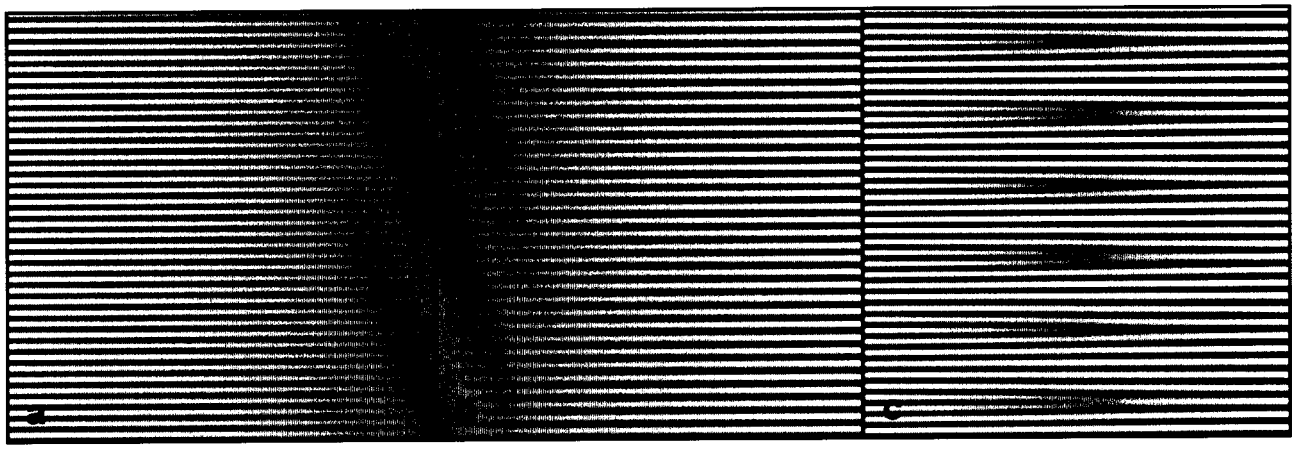

Figure 5. Computer simulation of two regions with different lattice constants but parallel (a, b) in order to explain figure 4. (c) Overlap of the two different regions with six step dislocations.

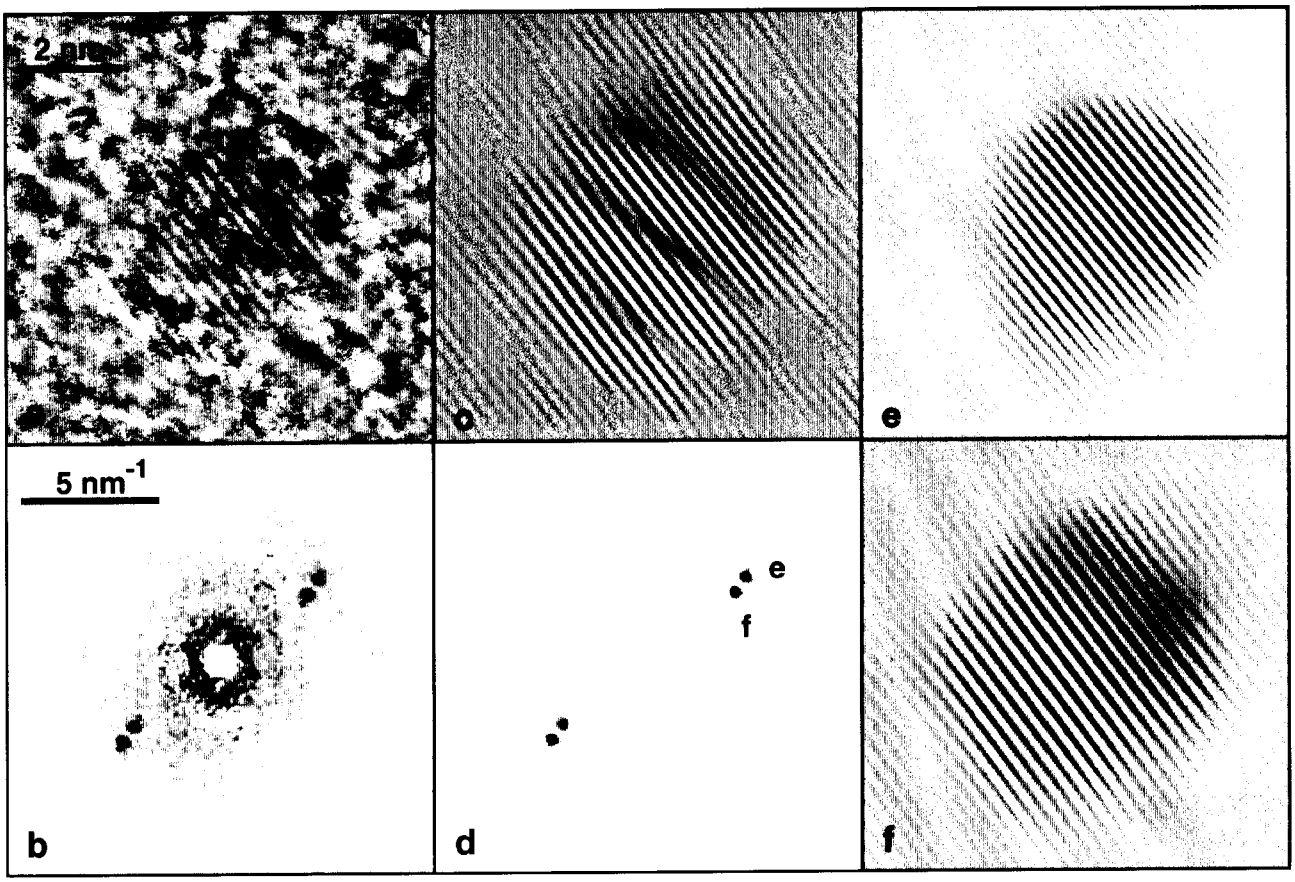

Figure 6. Transition between Cu and Cu_2O. Layered structure tilted by 2°. (a) Unfiltered image. (b) PS of the unfiltered image. (c) Filtered image with three step dislocations. (d) Ps of the filtered image. (e) Core region (assumed) of Cu, filtered. (f) Top and bottom region (assumed) of Cu_2O, filtered.

114 h. This consists of different regions which can be interpreted as a monoclinic tenorite structure of CuO in the [110] orientation with the −111 and 002 reflections displayed in the PS and of Cu_2O cuprite structure also in the [110]-orientation with the −11 −1, −110 and −111 reflections in the PS. However, because the particle consists of these two different oxides, they can only coexist by inserting deformations. This means that the monocli-

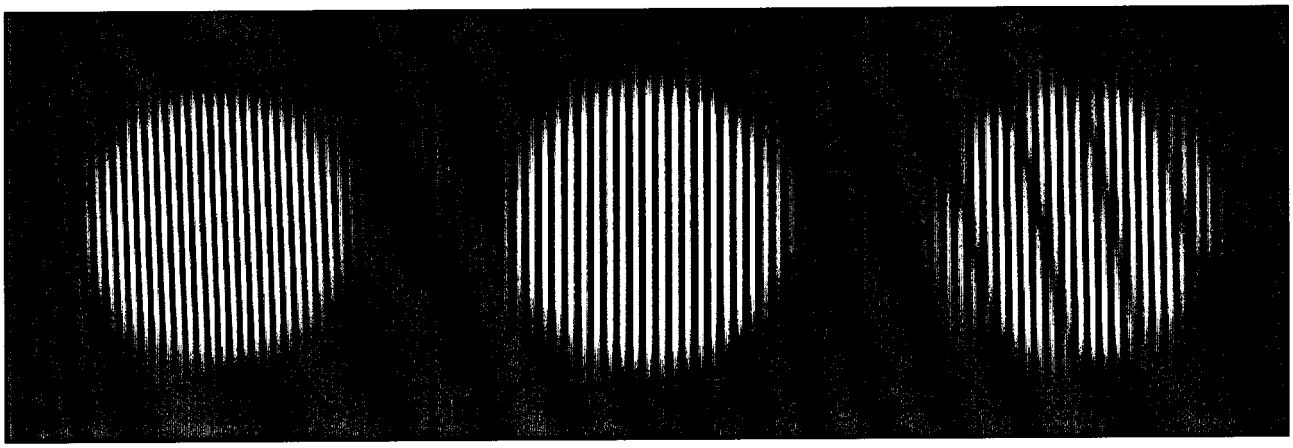

Figure 7. Computer simulation consisting of two layers tilted by 2° with different lattice constants (a, b) in order to explain figure 6. (c) Sum of layers a and b.

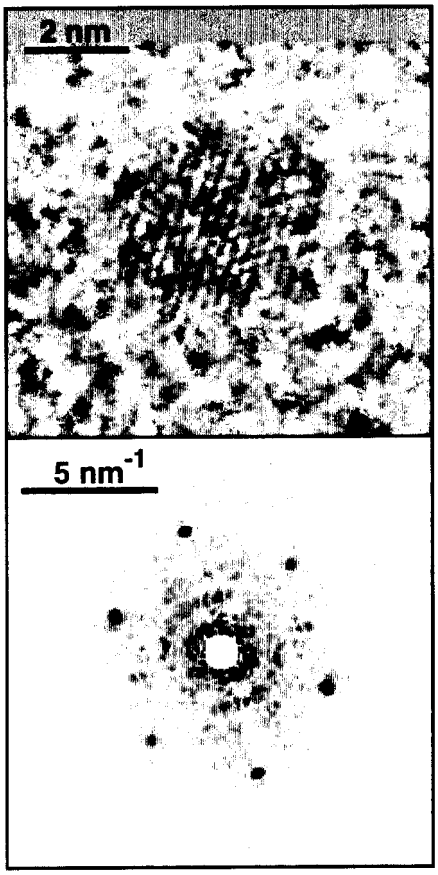

nic tenorite unit cell and the cubic cuprite unit cell are deformed. For the tenorite cell the following data can be obtained from the PS:

experimental	*bulk*
$a = 0.4694$ nm	$a = 0.4684$ nm
$b = 0.3418$ nm	$b = 0.3425$ nm
$c = 0.5411$ nm	$c = 0.5129$ nm
$\beta = 101.2°$	$\beta = 99.47°$

$$\Delta^2 = 7.97 \times 10^{-4}\ \text{nm}^2\,.$$

The cubic cuprite cell is deformed resulting in an orthorhombic cell:

$a = 0.3930$ nm	$a = b = c = 0.4270$ nm
$b = 0.4347$ nm	
$c = 0.4076$ nm	

$$\Delta^2 = 1.59 \times 10^{-3}\ \text{nm}^2\,.$$

Δ^2 is the mean square deviation of the cell parameters from the bulk data, i.e.:

Figure 8. Cu_2O cuprite in the [110]-orientation. The PS is shown in the lower part.

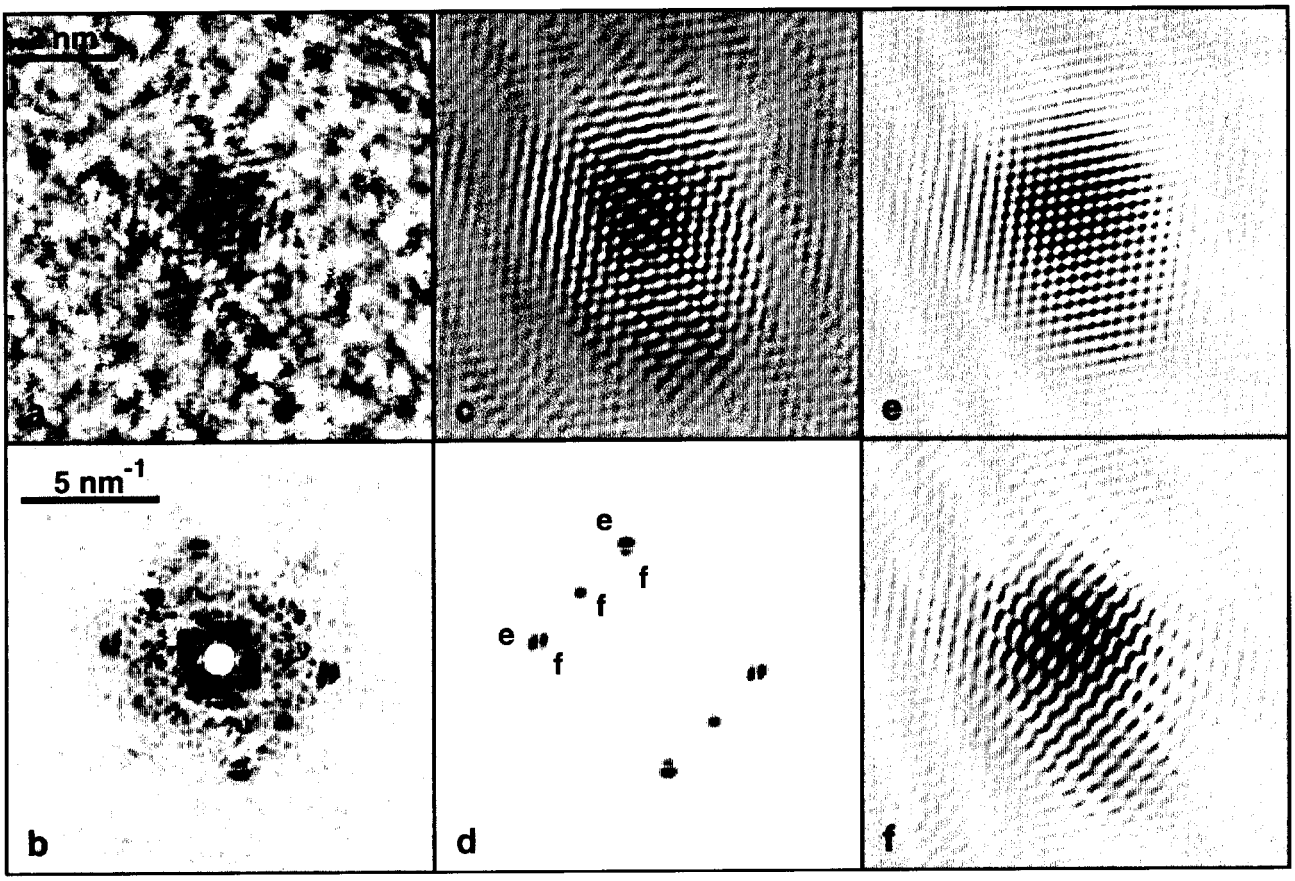

Figure 9. Coexistence of CuO (tenorite) and Cu_2O (cuprite) in the [110]-orientation. (a) Unfiltered image. (b) PS of the unfiltered image. (c) Filtered image. (d) PS of the filtered image. (e) Filtered image of tenorite. (f) Filtered image of cuprite.

$$\Delta^2 = \Delta a^2 + \Delta b^2 + \Delta c^2 .$$

Composite particles consisting of Cu, Cu_2O and Cu_xO_y regions in the same particle with distortions at the interfaces could be observed even after more than 100 h of storage in air at room temperature. Angles and lattice parameters suggest distortions due to the interface with the oxide.

References

[1] S.C. Jain, A.H. Harker and R.A. Cowley, Philos. Mag. A 75 (1997) 1461.
[2] V. Gnutzmann and W. Vogel, J. Phys. Chem. 94 (1990) 4991.
[3] W. Vogel, W.M.H. Sachtler and Z. Zhang, Ber. Bunsenges. Phys. Chem. 97 (1993) 280.
[4] N. Hartmann, R. Imbiehl and W. Vogel, Catal. Lett. 28 (1994) 373.
[5] C.G. Granqvist and J. Buhrman, J. Appl. Pys. 47 (1976) 2200.
[6] F. Frank, W. Schulze, B. Tesche, J. Urban and B. Winter, Surf. Sci. 156 (1985) 90.
[7] J. Urban, H. Sack-Kongehl and K. Weiss, Z. Phys. D 36 (1996) 73.
[8] J. Urban, H. Sack-Kongehl and K. Weiss, High Temp. Mater. Sci. 36 (1997) 155.
[9] B. Tesche, Vak. Tech. 24 (1975) 104.
[10] J.W. Mathews and W.M. Stobbs, Philos. Mag. 36 (1977) 373.
[11] G. Nihoul, Microsc. Microanal. Microstruct. 2 (1991) 637.
[12] S. Giorgio, G. Nihoul, J. Urban and H. Sack-Kongehl, Z. Phys. D 24 (1992) 395.
[13] P. Goodman and A.F. Moodie, Acta Cryst. A 30 (1974) 280.
[14] J. Urban, H. Sack-Kongehl and K. Weiss, Z. Phys. D 28 (1993) 247.